Chemical Science

EDGE ARTICLE

View Article Online
View Journal | View Issue

Check for updates

Cite this: *Chem. Sci.*, 2019, **10**, 4580

All publication charges for this article have been paid for by the Royal Society of Chemistry

Open Access Article. Published on 18 bezna 2019. Downloaded on 02.02.2026 20:22:41.
This article is licensed under a Creative Commons Attribution-NonCommercial 3.0 Unported Licence.

Photoinitiated carbonyl-metathesis: deoxygenative reductive olefination of aromatic aldehydes *via* photoredox catalysis†

Shun Wang, Nanjundappa Lokesh, Johnny Hioe, Ruth M. Gschwind* and Burkhard König*

Carbonyl–carbonyl olefination, known as McMurry reaction, represents a powerful strategy for the construction of olefins. However, catalytic variants that directly couple two carbonyl groups in a single reaction are less explored. Here, we report a photoredox-catalysis that uses B_2pin_2 as terminal reductant and oxygen trap allowing for deoxygenative olefination of aromatic aldehydes under mild conditions. This strategy provides access to a diverse range of symmetrical and unsymmetrical alkenes with moderate to high yield (up to 83%) and functional-group tolerance. To follow the reaction pathway, a series of experiments were conducted including radical inhibition, deuterium labelling, fluorescence quenching and cyclic voltammetry. Furthermore, NMR studies and DFT calculations were combined to detect and analyze three active intermediates: a cyclic three-membered anionic species, an α-oxyboryl carbanion and a 1,1-benzyldiboronate ester. Based on these results, we propose a mechanism for the C=C bond generation involving a sequential radical borylation, "bora-Brook" rearrangement, B_2pin_2-mediated deoxygenation and a boron-Wittig process.

Received 10th February 2019
Accepted 18th March 2019

DOI: 10.1039/c9sc00711c

rsc.li/chemical-science

Introduction

Alkenes are omnipresent in natural compounds and essential functional groups for many chemical transformations. Among many methods that have been developed for the generation of alkenes, olefination and metathesis reactions converting two functional groups into one alkene are particularly useful for the synthesis of complex molecules. The classic Wittig olefination uses phosphonium ylide reagents (Scheme 1A, eqn (1))[1] and many related carbonyl olefination processes, such as the Horner–Wadsworth–Emmons,[1b] Peterson,[2] Julia[3] and Tebbe[4] reactions utilizing different ylide or carbene precursors have been developed. Olefin cross-metathesis reactions catalyzed by metal alkylidenes allow the exchange between two olefins to form a pair of distinct alkenes (Scheme 1A, eqn (2)).[5] The related catalytic olefin–carbonyl metathesis strategy for the synthesis of alkenes was discovered just recently (Scheme 1A, eqn (3)).[6]

Contrary to these olefination and metathesis processes, catalytic bicarbonyl olefination reactions remain less developed. The McMurry reaction provides an attractive route to alkenes from two carbonyl groups (Scheme 1B).[7] The net result of such a carbonyl–carbonyl olefination could be viewed as a "metathesis" process although the oxygen atom is generally

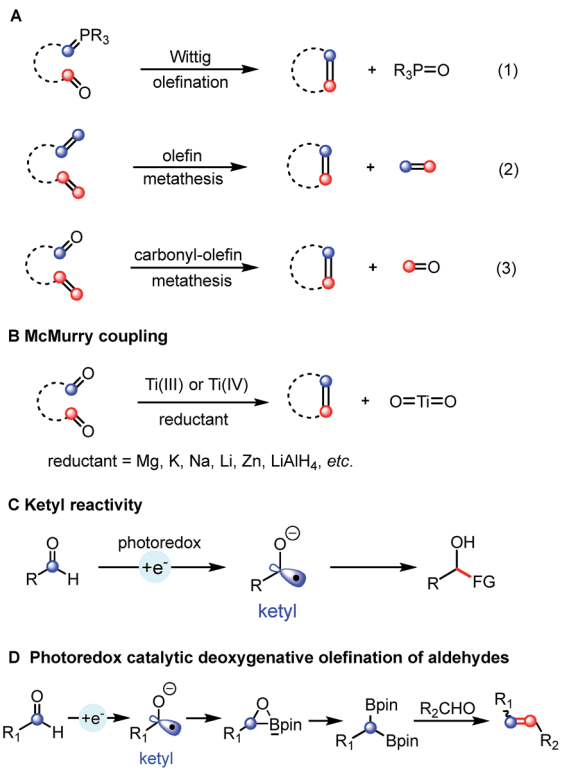

Scheme 1 Divergent functionalization of carbonyl.

Faculty of Chemistry and Pharmacy, University of Regensburg, D-93040 Regensburg, Germany. E-mail: ruth.gschwind@ur.de; burkhard.koenig@ur.de

† Electronic supplementary information (ESI) available. See DOI: 10.1039/c9sc00711c

This journal is © The Royal Society of Chemistry 2019

Open Access Article. Published on 18 bezna 2019. Downloaded on 02.02.2026 20:22:41.
This article is licensed under a Creative Commons Attribution-NonCommercial 3.0 Unported Licence.

not released as oxygen gas, but bounded to reagents. Classic McMurry protocols use titanium salts in combination with a reducing reagent under heating. The whole process is driven thermodynamically by the formation of strong Ti–O bonds. Despite being very effective and widely used, this system generally requires relatively harsh reaction conditions, such as the use of stoichiometric amounts of the titanium reagent and strong reductants at high temperature, lowering the overall functional group tolerance.[7,8] Therefore, several milder and catalytic methods were developed. A variant using only catalytic amounts of titanium with an excess of chlorosilane was developed by Fürstner and co-workers.[9] Wagner used hexachlorodisilane at high temperature (160 °C) for converting diarylmethanones into tetraarylethylenes.[10] More recently, Ott *et al.* reported the stereoselective preparation of *E*-alkenes from two aldehydes by using phosphanylphosphonate.[11] After that, Li described a stepwise Ru-catalyzed carbonyl–carbonyl olefination method wherein hydrazine was employed as the mediator to transform one carbonyl into its carbanion equivalent.[12] Despite these advances, the direct catalytic carbonyl–carbonyl olefination in one-step and under mild reaction conditions remains a challenge.

In recent years, photoredox catalysis has evolved into an attractive alternative to traditional strategies for generating radical intermediates.[13] For instance, ketyl radicals are easily accessed from carbonyl compounds by using a photoredox-mediated single-electron reduction strategy.[14] The obtained ketyl radicals have been used in C–C bond formation by addition to π systems or radical–radical coupling (Scheme 1C). However, a photoredox catalyzed reductive coupling of carbonyls followed by deoxygenation yielding a carbon–carbon double bond has not been achieved so far. Herein, we report the first deoxygenative olefination coupling of aromatic aldehydes enabled by the cooperative action of bis(pinacolato)diboron and a photoredox catalytic system (Scheme 1D).

The anticipated deoxygenative olefination process requires a four-electron reduction and an efficient oxygen acceptor. Moreover, a careful design of the catalytic system is required to suppress the competing pinacol coupling.[15] With these mechanistic challenges in mind, we envisioned the possibility of combining the photocatalytic carbonyl reduction system with a diboron reagent allowing an efficient McMurry-type process based on the following considerations: (1) the Lewis acidity of the boron atom of the diboronate compounds could potentially activate the carbonyl groups thus facilitating the single electron reduction process.[16] (2) The formation of a strong B–O bond would provide a significant thermodynamic driving force for the deoxygenation process.[16b,17]

Results and discussion

Optimization of reaction condition

To examine the feasibility of our hypothesis, we chose *para*-tolualdehyde **1a** as the model substrate in combination with bis(pinacolato)diboron (B_2pin_2) as the oxygen acceptor. A promising result was obtained when irradiating a mixture containing **1a**, B_2pin_2, DIPEA, Cs_2CO_3, $[Ir(dFCF_3ppy)_2dtbbpy]PF_6$ (1 mol%) and DMF with a blue LED lamp giving trace amounts of alkene **2a** (see ESI Table S1, entry 1†). Interestingly, removing the electron donor DIPEA from the system also yielded the product in 6% yield with full conversion of **1a** (Table S1, entry 2†). Moreover, the alkene **2a** was not detected in the absence of either Cs_2CO_3 or B_2pin_2 (Table S1, entry 3–4†). As the formation of the product does not require an additional electron donor, we reasoned that B_2pin_2 may serve as the terminal reductant and the oxygen acceptor in this reaction. Next, we explored the effect of another co-catalyst, which could potentially shuttle electrons from the boron species to the photocatalytic system.[18] To our delight, a significant increase in yield (39%, Table S1, entry 6†) was observed upon adding benzyl thiol (10 mol%) as co-catalyst, whereas quinuclidine proved ineffective (Table S1, entry 5†). Testing the reaction with other bases resulted in lower yields (Table S1, entry 7–15†). Further evaluation of other thiols revealed that only benzyl thiol (20 mol%) and 4-Me-benzyl thiol (20 mol%) gave comparably good yields (Table S2, entry 6 and 14†). A variety of photocatalysts were tested for this transformation; using a slightly modified catalyst $[Ir(FCF_3ppy)_2dtbbpy]PF_6$ increased the yield to 74% (Z/E = 2.2/1). Screening of the solvents revealed that DMF was the optimal solvent for this reaction (Table S3†). Better yield and Z/E selectivity were achieved by employing a combination of $[Ir(FCF_3ppy)_2dtbbpy]PF_6$ with 4-Me-benzyl thiol (Table S4, entry 3†). Subsequently, the effect of concentration was examined, subtle varying the concentration to 0.33 M increased the yield to 87% with a better Z/E selectivity of the product (Z/E = 2.6/1) (Table S5, entry 3†). Interestingly, small amounts of product **2a** (17%, Table 1, entry 10) were also detected in the absence of the photocatalyst. Presumably, a small amount of benzaldehyde is excited by visible light in the presence of B_2pin_2 to form ketyl radicals that lead to the formation of product. However, further control experiments confirmed that both the photocatalyst and light were crucial for an efficient transformation (Table 1, entry 9 and 10).

Synthetic scope

With the optimized reaction conditions in hand, we then investigated the scope of this reaction with substituted aromatic aldehydes as substrates (Fig. 1). A broad range of aromatic aldehydes bearing *para*-(**1a–1g**), *meta*-(**1h–1p**) or *ortho*-(**1q–1s**) substituents reacted smoothly to afford the corresponding alkenes. Many synthetically useful functional groups including alkyl (**1a**, **1c** and **1q**), alkoxyl (**1d–e**, **1h**, **1r** and **1t**), acetal (**1u**), silyl (**1m**), boronic ester (**1n**) are tolerated in this transformation.

Importantly, the presence of acidic protons in amides (**1f–g**, and **1i**) and amines (**1j**) did not interfere with the reaction, giving yields of the isolated alkenes ranging from 47% to 63%. Aromatic substituents, such as phenyl (**1k**, **1s**) and thiophenyl (**1l**) furnished alkene products, albeit in lower yields. Furthermore, the reaction was compatible with halogen substituents on the benzaldehydes and gave the chloro- and fluoro-substituted alkenes in 40% and 32% yield, respectively (**1o–p**). However, benzaldehydes possessing strong electron-withdrawing groups, such as nitro or nitrile, were not tolerated. *ortho*-Substituted 2-methyl benzaldehyde gave an excellent Z/E selectivity (Z/E: 16/1) and good yield (60%). More

Open Access Article. Published on 18 bezna 2019. Downloaded on 02.02.2026 20:22:41.
This article is licensed under a Creative Commons Attribution-NonCommercial 3.0 Unported Licence.

Table 1 Screening of reaction conditions[a]

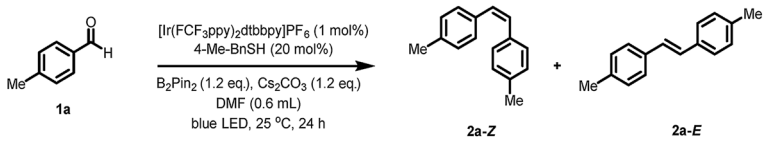

Entry	Change from standard conditions	Yield of **2a** (Z and E) [%]	Z/E[b]
1	None	87	2.6/1
2	Without thiol	Trace	—
3	Without B_2pin_2	0	—
4	Without Cs_2CO_3	Trace	—
5	Na_2CO_3 instead of Cs_2CO_3	Trace	—
6	CsF instead of Cs_2CO_3	Trace	—
7	DMF (1 mL)	77	2.5/1
8	DMF (0.4 mL)	68	2.4/1
9	Without light	0	—
10	Without photocatalyst	17	3.5/1

[a] Unless otherwise noted, all reactions were carried out with **1a** (0.2 mmol), $[Ir(FCF_3ppy)_2dtbbpy]PF_6$ (0.002 mmol), B_2pin_2 (0.24 mmol), Cs_2CO_3 (0.24 mmol), 4-Me-BnSH (0.04 mmol) in anhydrous DMF (0.6 mL) under nitrogen, irradiation with 3 W blue LED for 24 h at 25 °C. Yields were determined by crude NMR using 1,3,5-trimethoxybenzene as an internal standard. [b] $Z:E$ ratio determined by ^1H NMR analysis.

sterically hindered groups such as methoxy (**1r**) and phenyl (**1s**) at the *ortho*-position showed a similarly high Z/E selectivity up to (39 : 1), albeit a decreased yield. This significant increase in Z/E selectivity may be attributable to the increase in triplet energy of the Z isomers caused by a larger twisting angle in the presence of an *ortho*-substitution, while a small increase in triplet energy in the less-congested E isomer is expected.[19] Additionally, heteroarenes including benzothiophene (**1v**), benzofuran (**1w**) as well as indole (**1x**) performed well in this transformation. However, aliphatic aldehydes and aromatic ketones gave only trace amounts of products with low conversions, presumably due to their higher reduction potentials and steric hindrance, respectively.

After having established the scope of aldehydes in homo-coupling reactions, we turned our attention to more challenging cross-coupling reactions between two different aldehydes. As shown in Fig. 2, using slightly modified reaction conditions, the coupling between two different aldehydes proceeds well to give a range of unsymmetrical alkenes. Aldehydes bearing amides and amine groups at the aromatic ring react smoothly with *para*-tolualdehyde to give the corresponding alkenes in moderate to good yields (**5a–5c**). Aldehydes carrying alkoxy groups at the phenyl ring were tolerated under our reaction conditions, affording the alkenes in modest to good yields with modest Z/E selectivity (**5d–5f**). However, this cross-coupling reaction is sensitive to steric hindrance and *ortho*-substituents led to a decreased reactivity (**5e**). The reaction of heteroaromatic aldehydes furnished a heterocycle-containing stilbene (**5g**). Coupling between benzaldehyde and 3,5-dimethoxybenzaldehyde afforded the alkene in 57% yield with good selectivity ($Z/E = 1/3.5$).[20]

Mechanistic investigation

To gain insights into the reaction mechanism, a series of chemical experiments, spectroscopic investigations and *in situ* illumination NMR experiments[21] were conducted.

The initial Stern–Volmer luminescence quenching experiments revealed that phenylmethanethiolate quenches the excited state of the photocatalyst much more efficiently than the corresponding thiol, while the aldehyde and B_2pin_2 do not quench at all (see ESI, Fig. S6†). This indicates a potential electron transfer from the sulfur anion to the excited state of the photocatalyst. This reduced $[Ir(FCF_3ppy)_2dtbbpy]PF_6$ (II) ($Ir^{III/II}_{1/2} = -1.38$ V *vs.* SCE in DMF, Fig. S1†) catalyst causes the single electron reduction of **1a**. Even though the E_{red} of **1a** is higher ($E_{red} = -2.07$ V *vs.* SCE in DMF, Fig. S3†), the decrease of reduction potential of aldehyde **1a** on addition of Lewis acidic B_2pin_2 (Fig. S4 and S5†) facilitates this single-electron reduction.

Next, the presence of radical species in the catalytic cycle was tested by addition of 2,2,6,6-tetramethylpiperidin-1-oxyl (TEMPO, 1.0 eq.) to the mixture, which shows a dramatic drop in product yield (down to 8% see ESI†). This was also evidenced in the ^{13}C NMR spectrum, which shows a line broadened signal for the carbonyl of the benzaldehyde (see ESI Fig. S9†), possibly due to exchange of the radical species (ketyl radical) with benzaldehyde.

Subsequently, a series of control experiments were performed to identify key intermediates. 1,2-Diol, benzyl alcohol and 1,2-diketone were excluded as intermediates, since using them in place of benzaldehyde did not lead to alkene formation (ESI, Scheme S1†). Furthermore, benzylboronic esters **S4** and benzyloxyborate ester **S5** were identified as by-products in the reaction (Fig. S7†). Most interestingly, control experiments in the presence of D_2O (10.0 eq.) quenched the reaction

 This journal is © The Royal Society of Chemistry 2019

Open Access Article. Published on 18 bezna 2019. Downloaded on 02.02.2026 20:22:41.
This article is licensed under a Creative Commons Attribution-NonCommercial 3.0 Unported Licence.

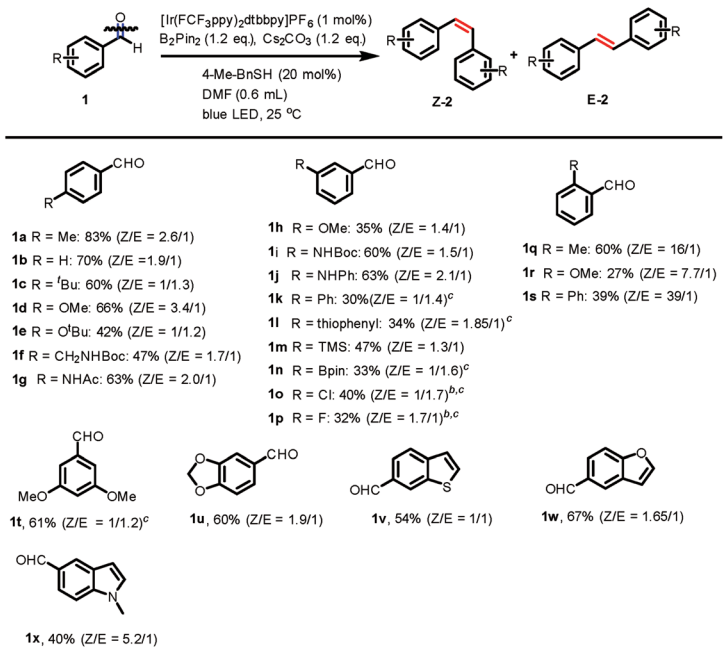

Fig. 1 Scope of aldehydes for the homo-coupling deoxygenative olefination[a]. [a]Reaction conditions: **1** (0.2 mmol), $[Ir(FCF_3ppy)_2dtbbpy]PF_6$ (0.002 mmol), B_2pin_2 (0.24 mmol), Cs_2CO_3 (0.24 mmol), 4-MeBnSH (0.04 mmol) in anhydrous DMF (0.6 mL), irradiation with 3 W blue LED for 24 h at 25 °C, isolated yields. Yields are the combined yield of *Z* and *E* isomers. [b]Ethyl 2-mercaptopropionate (0.04 mmol) was used in place of 4-MeBnSH. [c]Isolated yield, average of two parallel reactions.

significantly, affording the alkene in trace amounts along with the formation of deuterated (at the benzylic position) boronic esters **S4-D** and borate ester **S5-D** (Scheme 2). In contrast, with only d^7-DMF as solvent, deuterium was not incorporated in the products or the boronic ester **S4** and borate ester **S5**. These findings suggest intermediate boron-related species, such as an α-oxyboryl carbanion[22] and an α-boryl carbanion[23] in the reaction mechanism.

Next, a systematic *in situ* illumination NMR study was carried out to directly detect these reaction intermediates. To monitor this unusual transformation from carbonyl groups to double bonds and to boost sensitivity of otherwise insensitive ^{13}C signals, benzaldehyde specifically ^{13}C labelled at the carbonyl position was used (see Fig. 3A). This enabled us not only to predominately track the chemical modulations at the carbonyl position, but also to identify the number of protons bound to the carbon in several intermediate species by ^1H coupled 1D ^{13}C experiments (see below); therefore, in the following only the ^{13}C signals of the labelled carbon are discussed.

On irradiation (455 nm, blue LED) of the reaction mixture, besides starting material and product resonances, several new ^{13}C signals are detected, indicating the generation of possible reaction intermediates. Fig. 3A shows the *in situ* ^1H decoupled ^{13}C spectrum of the reaction mixture after 18 hours of

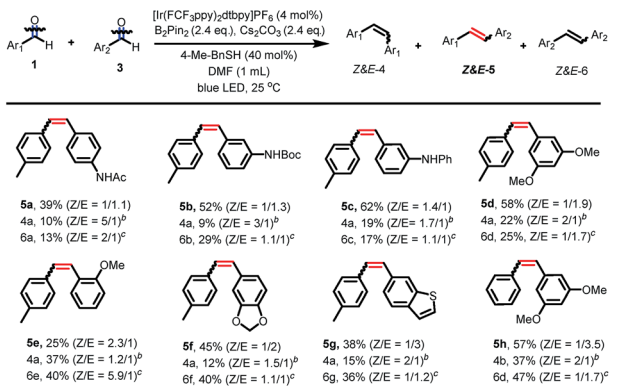

Fig. 2 Scope of aldehydes for the cross-coupling deoxygenative olefination[a]. [a]Reaction conditions: **1** (0.1 mmol), **3** (0.15 mmol), $[Ir(FCF_3ppy)_2dtbbpy]PF_6$ (0.004 mmol), B_2pin_2 (0.24 mmol), Cs_2CO_3 (0.24 mmol), 4-Me-BnSH (0.04 mmol) in anhydrous DMF (1 mL), irradiation with 3 W blue LED for 24 h at room temperature, isolated average yield of two parallel reactions. Yields refer to the combined yield of *Z* and *E* isomers. [b]Yields and *Z*/*E* ratio values were determined with ^1H NMR using 1,3,5-methoxybenzene as internal standard; based on the amount of aldehyde **1**. [c]Yields and *Z*/*E* ratio values were determined with ^1H NMR using 1,3,5-methoxybenzene as internal standard; based on the amount of aldehyde **3**.

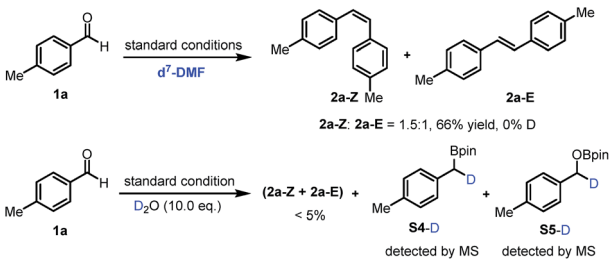

Scheme 2 Deuteration experiments.

Open Access Article. Published on 18 bezna 2019. Downloaded on 02.02.2026 20:22:41.
This article is licensed under a Creative Commons Attribution-NonCommercial 3.0 Unported Licence.

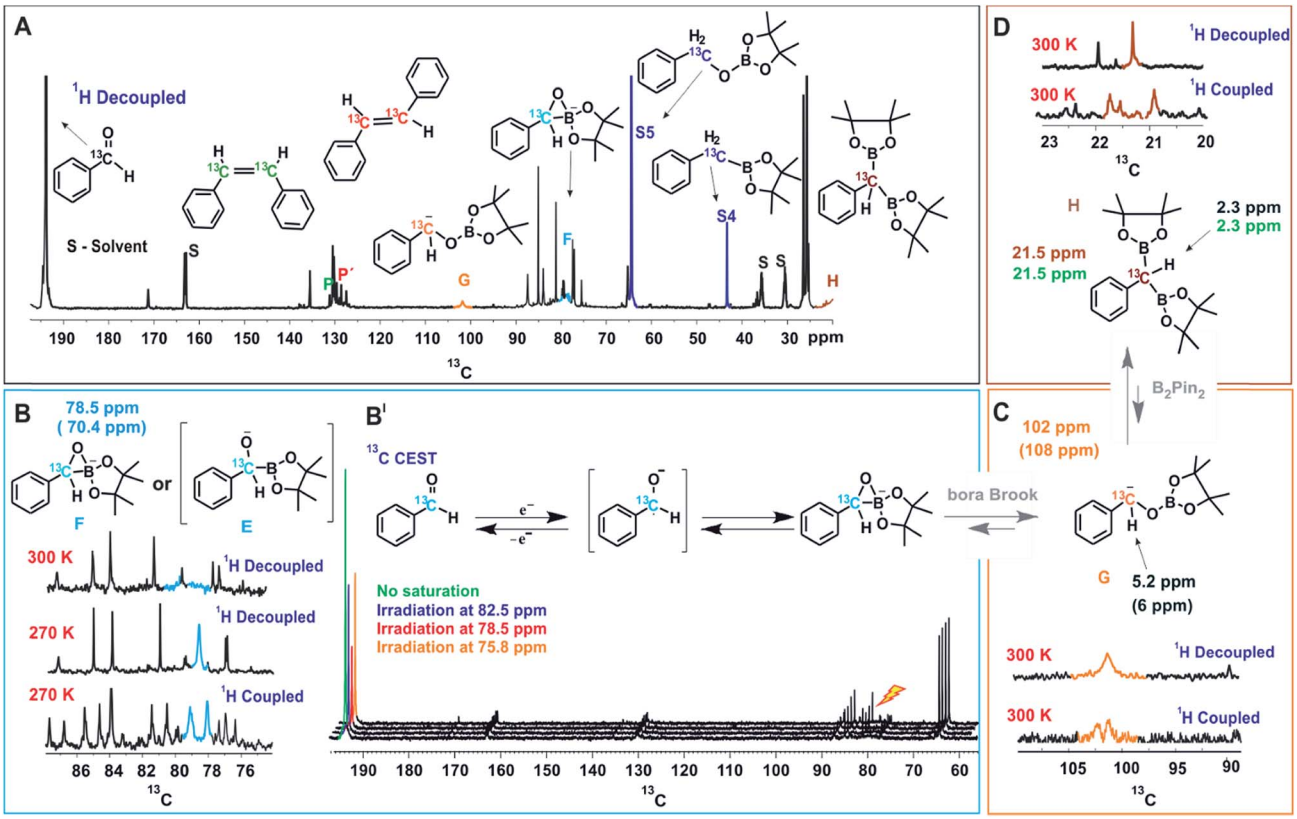

Fig. 3 NMR Studies of the Reaction Intermediates. (A) *In situ* ^{13}C spectrum of the reaction mixture after 18 hours of illumination, the observed intermediate peaks are marked with respective colors and stable intermediates are directly compared to independently synthesized compounds. (B) Stabilization and characterization of transient intermediate **F** is achieved at low temperature (270 K) and characterized from ^{1}H decoupled and coupled ^{13}C spectra. (B′) ^{13}C CEST spectra establishing initial chemical transformation between benzaldehyde and primary key intermediate **F**. (C) Identification of α-oxyboryl carbanion **G** from ^{13}C and ^{1}H chemical shifts (for HSQC see ESI†) and the multiplicity pattern of ^{13}C at the benzylic position. (D) Assignment of intermediate **H** from the multiplicity pattern of ^{13}C at the benzylic position and ^{13}C and ^{1}H chemical shifts (for HSQC see ESI†). The ^{1}H and ^{13}C chemical shifts of independently synthesized **H** are given in green. The values inside brackets are calculated chemical shift values. Unless otherwise mentioned, all spectra were measured at 300 K, in a 600 MHz NMR spectrometer.

irradiation. Besides benzaldehyde, the two products (**P** and **P′** in Fig. 3A), and the by-products **S4** and **S5**, several additional peaks appeared. Among them three intermediates were assigned, which are marked with **G**, **F** and **H** and highlighted with different colors in Fig. 3A. To identify and characterize the intermediates, a combined approach of chemical exchange information from ^{13}C CEST (chemical exchange saturation transfer), chemical shift information and multiplicity pattern accessed from ^{1}H coupled 1D ^{13}C spectra was applied. Furthermore, theoretical calculations and spectra of individually synthesized intermediates were used to corroborate the assignment.

To identify the next intermediate formed from benzaldehyde, the spectra are scanned by ^{13}C CEST NMR (detailed information about CEST is given in ESI†).[24] In case there is any chemical exchange on the ms time scale with benzaldehyde, saturation can be transferred from the exchanging intermediate onto benzaldehyde and hence the intermediate becomes detectable. The most pronounced intensity drop observed for the benzaldehyde ^{13}C═O signal at 193 ppm is on saturation at 78.5 ppm (Fig. 3B′). However, at 300 K, the peak at 78.5 ppm is very broad (blue, Fig. 3B) suggesting a transient nature of the intermediate. To characterize this intermediate further, the temperature was lowered to 270 K resulting in a considerable narrowing of this ^{13}C signal. In addition, the ^{1}H coupled ^{13}C spectrum reveals a ^{13}C–H moiety by appearance of a doublet. From the literature, it was considered that the base might react with the diboron reagent to generate sp^3–sp^2 diboron species that participates in ketyl radical borylation[25] to give α-boryl alkoxide. Furthermore, theoretical calculations predict a ^{13}C chemical shift of 70.4 ppm for a cyclic three-membered anionic species **F** (Fig. 3B). The open form of the α-boryl alkoxide **E** was found to be energetically less favorable by theoretical calculations. However we cannot distinguish experimentally between **E** and **F**. Based on this evidence, the ^{13}C peak at 78.5 ppm is assigned to the cyclic three-membered species **F** or to the α-boryl carbonyl peak of benzaldehyde indicate a fast chemical alkoxide **E**; thus, the above discussed line broadening of exchange with the ketyl radical. In addition, CEST exchange saturation transfer reveals a slow exchange of benzaldehyde with the cyclic three-membered anionic species **F** or **E**. Combining the experimental observations we conclude that a sequential exchange process takes place from benzaldehyde through a very short-lived ketyl radical to **E** or **F**.

 This journal is © The Royal Society of Chemistry 2019

Open Access Article. Published on 18 bezna 2019. Downloaded on 02.02.2026 20:22:41.
This article is licensed under a Creative Commons Attribution-NonCommercial 3.0 Unported Licence.

Next, the assignment of the α-oxyboryl carbanion intermediate **G** is discussed (see Fig. 3C). In a "bora-Brook" rearrangement process this α-oxyboryl carbanion **G** was found to be generated from the isomerization of α-boryl alkoxide **E**.[22] Furthermore, Nozaki *et al.* proposed a three-membered-ring species similar to **F** as the transition state of the C to O boryl migration in the "bora-Brook" rearrangement.[22c] Given these reports and the oxophilicity of boron (B–O bond BDE = 193 kcal mol^{-1}),[26] such a carbon to oxygen boryl migration in the cyclic three-membered anionic species **F** to generate α-oxyboryl carbanion **G** is highly probable. The aforementioned control experiments, wherein deuterium-trapped benzyloxyborate ester **S5-D** was observed, further corroborates the existence of **G**. Indeed, we could detect a relatively broad peak of very small intensity at 102 ppm in the reaction mixture corresponding to the benzylic carbon of α-oxyboryl carbanion **G** (Fig. 3A and C). The ^{1}H coupled ^{13}C spectrum shows a doublet (Fig. 3C) indicating a ^{13}CH group and the calculated chemical shifts (^{13}C 108 ppm and ^{1}H 6 ppm) are in good agreement with the assignment to the benzylic carbon of α-oxyboryl carbanion **G**. Moreover, the essential role of DMF and Cs_2CO_3 in our reaction is in line with the observation by Nozaki that the presence of a polar solvent and larger alkali metal cation could enhance the nucleophilicity of the anionic oxygen atom in such processes.[22c] Overall, we conclude that the α-oxyboryl carbanion **G** is generated *via* a "bora-Brook" rearrangement from the cyclic three-membered anionic species **F**.

Previous theoretical calculations showed that the transformation of an α-oxyboryl carbanion **G** to a 1,1-benzyldiboronate ester **H** (for structure see Fig. 3D) is thermodynamically and kinetically favorable.[27] Therefore, the intermediacy of **H** in our reaction process was examined with NMR. To identify the chemical shifts of **H**, a ^{13}C–^{1}H HSQC spectrum (see, ESI†) of the pure independently synthesized intermediate **H** was measured and revealed a benzylic carbon at 21.5 ppm and the corresponding proton at 2.50 ppm. Indeed, careful observation of the ^{13}C spectra of the reaction mixture revealed a very small peak of **H** at 21.5 ppm (Fig. 3A and D). The assignment to **H** was confirmed by a doublet (–^{13}CH) in the ^{1}H coupled ^{13}C spectrum (Fig. 3D) and HSQC spectra of the reaction mixture (ESI†). At present, we can only suggest that **H** is formed *via* a nucleophilic attack of the carbanion **G** to B_2pin_2 followed by a deoxygenation step. A related mechanism was proposed by Liu and Lan *et al.* for a borylation of an α-oxyboronic species, in which similar *gem*-diboron compounds are generated *via* an oxoanion instead of a carbanion attacking B_2pin_2.[27]

gem-Diborylalkanes, such as intermediate **H**, treated with a suitable base, are known to be deprotonated or monodeborylated to boryl carbanions.[23a–d,g] The resulting α-boryl anions react with carbonyl groups through a boron-Wittig pathway to give olefins.[23a–d,g] Indeed, the olefinic product could be obtained in an independent experiment treating benzaldehyde **1d** with 1,1-benzyldiboronate ester **H** in the presence of Cs_2CO_3 (Scheme 3A). Moreover, we could trap the α-boryl anion as boronic esters **S4-D** in the presence of D_2O (10.0 eq.) (Scheme 2). This is a strong hint that an α-boryl carbanion is involved in our reaction pathway, although we could not directly identify it *via in situ* NMR.

2,2′-Diphenyldicarboxaldehyde **1y** was used to investigate a potential intramolecular olefination reaction, but 9-phenanthrenol **2y′** was isolated as the main product (72%) with only 3% of phenanthrene **2y** (Scheme 3B; for more details, see ESI†).

Next, we turned our attention to explore the origin of the *Z*/*E* selectivity in the reaction. By NMR, we observed that the more thermodynamically stable *E* isomer was formed dominantly at the early stage of the reaction. Later, a *E* to *Z* isomerization occurs, with the *Z* isomer being the major product (Table S8†). We rationalize the formation of *E*-alkenes as the major configuration at the early reaction stage as a consequence of a *syn* boron–oxygen elimination.[23a,28] Additional evidence for the photo-induced alkene isomerization process was obtained when *E*-alkene was subjected to the standard reaction condition. The corresponding product was obtained in a similar *Z*/*E* ratio (*Z*/*E* = 2.6/1, 96% yield) as in our reaction system (Scheme 4A).[29] We also found that alkene *E*-**2a** could be obtained in one pot using the reported photo-sensitized *Z* to *E* isomerization strategy, giving alkene *E*-**2a** in 77% (Scheme 4B).[30]

Based on the above experimental evidence and mechanistic pathways previously reported in literature, we propose the mechanism depicted in Scheme 5 for the reported photocatalytic carbonyl–carbonyl olefination of aromatic aldehydes. Initially, the photoexcited state of $[Ir^{III}(FCF_3ppy)_2dtbbpy]^+$ is reductively quenched by the sulfur anion **A**, formed by the deprotonation of thiol by base, affording sulfur radical **B** and $[Ir^{II}(FCF_3ppy)_2dtbbpy]$ ($Ir^{III/II}_{1/2}$ = −1.38 V *vs.* SCE in DMF). Single electron transfer (SET) from the Ir(II) species to benzaldehyde in the presence of B_2pin_2 gives the ground-state Ir(III) and ketyl radical **C**. Subsequent radical borylation[31] of **C** produces radical anion **D** and anion **E** or **F**. The resulting radical

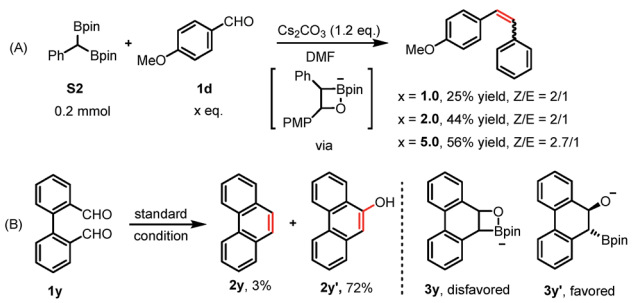

Scheme 3 Further mechanistic studies.

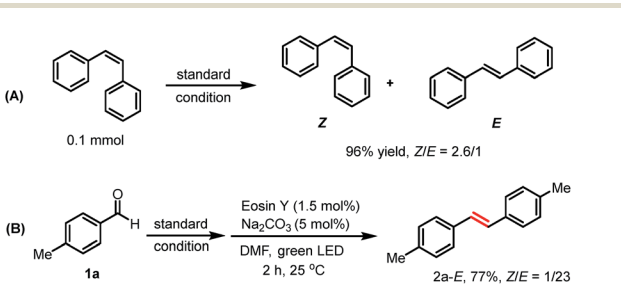

Scheme 4 Isomerization studies.

Open Access Article. Published on 18 bezna 2019. Downloaded on 02.02.2026 20:22:41.
This article is licensed under a Creative Commons Attribution-NonCommercial 3.0 Unported Licence.

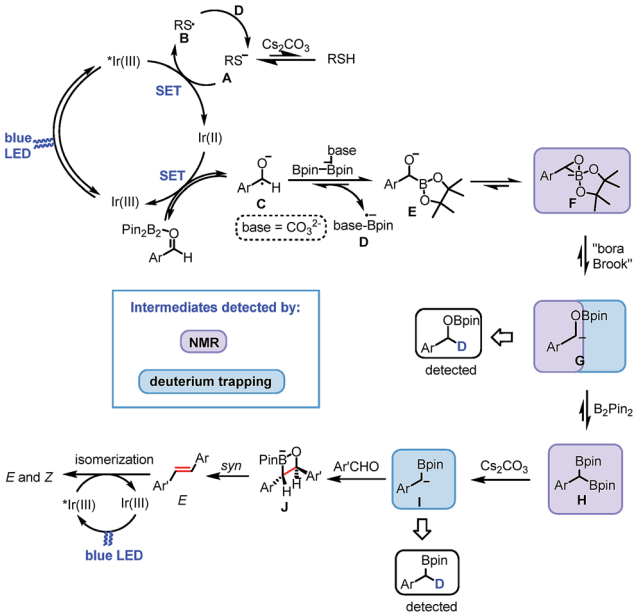

Scheme 5 Proposed reaction mechanism.

anion **D** reduces the sulfur radical **B** back to the anion **A**. The three-membered cyclic anion **F** undergoes a "bora-Brook" rearrangement to form α-oxyboryl carbanion **G**. The resulting carbanion **G** subsequently reacts with another molecule of B_2pin_2 leading to the formation of 1,1-benzyldiboronate ester **H**. The base-promoted mono-deborylation of **H** gives rise to the formation of α-boryl carbanion **I**. After nucleophilic attack to the carbonyl group of a second aldehyde, a four-membered cyclic intermediate **J** is most probably formed, which affords *E*-alkene *via* a B–O *syn* elimination. Finally, energy transfer from the excited state of the photocatalyst to the *E*-alkene produces a mixture of *Z* and *E* isomers as the final product.

Conclusions

In summary, we have developed a photoredox-catalyzed reaction for reductive carbonyl–carbonyl olefination of aromatic aldehydes using B_2pin_2 as both the oxygen atom trap and the terminal reductant. The reaction system provides a mild and efficient method to prepare both symmetrical and unsymmetrical diarylalkenes through intermolecular bicarbonyl olefination and tolerates a broad range of functional groups. Combining our *in situ* illumination NMR technique with a series of mechanistic studies, α-oxyboryl carbanion, α-boryl carbanion and 1,1-benzyldiboronate esters were detected as key intermediate species in the reaction. Furthermore, theoretical calculations corroborate the NMR observation of the cyclic three-membered anionic species involved in the "bora-Brook" rearrangement. Mechanistic studies support the hypothesis that the formation of the double bond is facilitated by a boron-Wittig process. This combination of photoredox catalysis with boron chemistry constitutes a unique example of an Umpolung strategy to convert an aldehyde into a boryl-functionalized carbanion.

Conflicts of interest

There are no conflicts to declare.

Acknowledgements

This work was supported by the German Science Foundation (DFG) (GRK 1626, Chemical Photocatalysis; KO 1537/18-1). This project has received funding from the European Research Council (ERC) under the European Unions Horizon 2020 research and innovation programme (grant agreement No. 741623). S. W. thanks the China Scholarship Council (CSC) for a predoctoral fellowship (CSC student number 201606280052). N. L. acknowledges ERC (ERC CoG-614182 – IonPairsAtCatalysis) for the funding. We are grateful to Dr Gregory S. Huff (University of Regensburg) for helpful discussions and writing suggestions. We further thank Dr Rudolf Vasold (University of Regensburg) for his assistance in GC-MS measurements and Ms Regina Hoheisel (University of Regensburg) for her assistance in cyclic voltammetry measurements.

Notes and references

1 (*a*) T. Takeda, *Modern carbonyl olefination: Methods and applications*, John Wiley & Sons, 2006; (*b*) B. E. Maryanoff and A. B. Reitz, *Chem. Rev.*, 1989, **89**, 863–927.
2 D. J. Peterson, *J. Org. Chem.*, 1968, **33**, 780–784.
3 J. B. Baudin, G. Hareau, S. A. Julia and O. Ruel, *Tetrahedron Lett.*, 1991, **32**, 1175–1178.
4 F. N. Tebbe, G. W. Parshall and G. S. Reddy, *J. Am. Chem. Soc.*, 1978, **100**, 3611–3613.
5 (*a*) A. H. Hoveyda and A. R. Zhugralin, *Nature*, 2007, **450**, 243; (*b*) O. Eivgi and N. G. Lemcoff, *Synthesis*, 2018, **50**, 49–63; (*c*) Y. Vidavsky and N. G. Lemcoff, *Beilstein J. Org. Chem.*, 2010, **6**, 1106–1119.
6 (*a*) J. R. Ludwig and C. S. Schindler, *Synlett*, 2017, **28**, 1501–1509; (*b*) L. Ravindar, R. Lekkala, K. P. Rakesh, A. M. Asiri, H. M. Marwani and H.-L. Qin, *Org. Chem. Front.*, 2018, **5**, 1381–1391; (*c*) M. R. Becker, R. B. Watson and C. S. Schindler, *Chem. Soc. Rev.*, 2018, **47**, 7867–7881.
7 J. E. McMurry, *Chem. Rev.*, 1989, **89**, 1513–1524.
8 A. Fürstner and B. Bogdanović, *Angew. Chem., Int. Ed. Engl.*, 1996, **35**, 2442–2469.
9 A. Fürstner and A. Hupperts, *J. Am. Chem. Soc.*, 1995, **117**, 4468–4475.
10 M. Moxter, J. Tillmann, M. Füser, M. Bolte, H.-W. Lerner and M. Wagner, *Chem.–Eur. J.*, 2016, **22**, 16028–16031.
11 K. Esfandiarfard, J. Mai and S. Ott, *J. Am. Chem. Soc.*, 2017, **139**, 2940–2943.
12 W. Wei, X.-J. Dai, H. Wang, C. Li, X. Yang and C.-J. Li, *Chem. Sci.*, 2017, **8**, 8193–8197.
13 (*a*) J. M. R. Narayanam and C. R. J. Stephenson, *Chem. Soc. Rev.*, 2011, **40**, 102–113; (*b*) J. Xuan and W.-J. Xiao, *Angew. Chem., Int. Ed.*, 2012, **51**, 6828–6838; (*c*) C. K. Prier, D. A. Rankic and D. W. C. MacMillan, *Chem. Rev.*, 2013, **113**, 5322–5363; (*d*) N. A. Romero and D. A. Nicewicz, *Chem. Rev.*, 2016, **116**, 10075–10166; (*e*) M. H. Shaw,

This journal is © The Royal Society of Chemistry 2019

Open Access Article. Published on 18 bezna 2019. Downloaded on 02.02.2026 20:22:41.
This article is licensed under a Creative Commons Attribution-NonCommercial 3.0 Unported Licence.

J. Twilton and D. W. C. MacMillan, *J. Org. Chem.*, 2016, **81**, 6898–6926; (*f*) D. Ravelli, S. Protti and M. Fagnoni, *Chem. Rev.*, 2016, **116**, 9850–9913; (*g*) K. L. Skubi, T. R. Blum and T. P. Yoon, *Chem. Rev.*, 2016, **116**, 10035–10074; (*h*) L. Marzo, S. K. Pagire, O. Reiser and B. König, *Angew. Chem., Int. Ed.*, 2018, **57**, 10034–10072.

14 (*a*) H. G. Yayla and R. R. Knowles, *Synlett*, 2014, **25**, 2819–2826; (*b*) E. C. Gentry and R. R. Knowles, *Acc. Chem. Res.*, 2016, **49**, 1546–1556; (*c*) N. Hoffmann, *Eur. J. Org. Chem.*, 2017, **2017**, 1982–1992; (*d*) K. N. Lee and M.-Y. Ngai, *Chem. Commun.*, 2017, **53**, 13093–13112.

15 M. Nakajima, E. Fava, S. Loescher, Z. Jiang and M. Rueping, *Angew. Chem., Int. Ed.*, 2015, **54**, 8828–8832.

16 (*a*) L. Deloux and M. Srebnik, *Chem. Rev.*, 1993, **93**, 763–784; (*b*) A. Maity and T. S. Teets, *Chem. Rev.*, 2016, **116**, 8873–8911; (*c*) E. Dimitrijević and M. S. Taylor, *ACS Catal.*, 2013, **3**, 945–962; (*d*) K. Ishihara and H. Yamamoto, *Eur. J. Org. Chem.*, 1999, **1999**, 527–538.

17 (*a*) D. S. Laitar, P. Müller and J. P. Sadighi, *J. Am. Chem. Soc.*, 2005, **127**, 17196–17197; (*b*) S. Bae and M. K. Lakshman, *J. Org. Chem.*, 2008, **73**, 1311–1319; (*c*) V. Gurram, H. K. Akula, R. Garlapati, N. Pottabathini and M. K. Lakshman, *Adv. Synth. Catal.*, 2015, **357**, 451–462; (*d*) J. Kim and C. R. Bertozzi, *Angew. Chem., Int. Ed.*, 2015, **54**, 15777–15781; (*e*) H. Lu, Z. Geng, J. Li, D. Zou, Y. Wu and Y. Wu, *Org. Lett.*, 2016, **18**, 2774–2776; (*f*) K. Yang, F. Zhou, Z. Kuang, G. Gao, T. G. Driver and Q. Song, *Org. Lett.*, 2016, **18**, 4088–4091; (*g*) M. Rauser, C. Ascheberg and M. Niggemann, *Angew. Chem., Int. Ed.*, 2017, **56**, 11570–11574; (*h*) W. Fu and Q. Song, *Org. Lett.*, 2018, **20**, 393–396.

18 (*a*) D. A. Nicewicz and D. S. Hamilton, *Synlett*, 2014, **25**, 1191–1196; (*b*) N. A. Romero and D. A. Nicewicz, *J. Am. Chem. Soc.*, 2014, **136**, 17024–17035; (*c*) M. Weiser, S. Hermann, A. Penner and H.-A. Wagenknecht, *Beilstein J. Org. Chem.*, 2015, **11**, 568–575.

19 (*a*) Y.-P. Zhao, L.-Y. Yang and R. S. H. Liu, *Green Chem.*, 2009, **11**, 837–842; (*b*) W. Cai, H. Fan, D. Ding, Y. Zhang and W. Wang, *Chem. Commun.*, 2017, **53**, 12918–12921; (*c*) X.-J. Wei, W. Boon, V. Hessel and T. Noël, *ACS Catal.*, 2017, **7**, 7136–7140; (*d*) K. Singh, S. J. Staig and J. D. Weaver, *J. Am. Chem. Soc.*, 2014, **136**, 5275–5278.

20 However, in all cases, the homo-coupled products of two aldehydes were observed (the yields were given in Table 2).

21 (*a*) C. Feldmeier, H. Bartling, E. Riedle and R. M. Gschwind, *J. Magn. Reson.*, 2013, **232**, 39–44; (*b*) C. Feldmeier, H. Bartling, K. Magerl and R. M. Gschwind, *Angew. Chem., Int. Ed.*, 2015, **54**, 1347–1351; (*c*) H. Bartling, A. Eisenhofer, B. König and R. M. Gschwind, *J. Am. Chem. Soc.*, 2016, **138**, 11860–11871.

22 (*a*) D. S. Matteson, *Aust. J. Chem.*, 2011, **64**, 1425–1429; (*b*) D. S. Matteson, *J. Org. Chem.*, 2013, **78**, 10009–10023; (*c*) H. Kisu, H. Sakaino, F. Ito, M. Yamashita and K. Nozaki, *J. Am. Chem. Soc.*, 2016, **138**, 3548–3552.

23 (*a*) I. Marek and J.-F. Normant, *Chem. Rev.*, 1996, **96**, 3241–3268; (*b*) T. Klis, S. Lulinski and J. Serwatowski, *Curr. Org. Chem.*, 2010, **14**, 2549–2566; (*c*) R. Nallagonda, K. Padala and A. Masarwa, *Org. Biomol. Chem.*, 2018, **16**, 1050–1064; (*d*) C. Wu and J. Wang, *Tetrahedron Lett.*, 2018, **59**, 2128–2140; (*e*) K. Hong, X. Liu and J. P. Morken, *J. Am. Chem. Soc.*, 2014, **136**, 10581–10584; (*f*) A. Noble, R. S. Mega, D. Pflästerer, E. L. Myers and V. K. Aggarwal, *Angew. Chem., Int. Ed.*, 2018, **57**, 2155–2159; (*g*) N. Miralles, R. J. Maza and E. Fernández, *Adv. Synth. Catal.*, 2018, **360**, 1306–1327.

24 N. Lokesh, A. Seegerer, J. Hioe and R. M. Gschwind, *J. Am. Chem. Soc.*, 2018, **140**, 1855–1862.

25 (*a*) A. Fawcett, J. Pradeilles, Y. Wang, T. Mutsuga, E. L. Myers and V. K. Aggarwal, *Science*, 2017, **357**, 283–286; (*b*) D. Hu, L. Wang and P. Li, *Org. Lett.*, 2017, **19**, 2770–2773; (*c*) L. Candish, M. Teders and F. Glorius, *J. Am. Chem. Soc.*, 2017, **139**, 7440–7443; (*d*) Y. Cheng, C. Mück-Lichtenfeld and A. Studer, *J. Am. Chem. Soc.*, 2018, **140**, 6221–6225; (*e*) J. Wu, L. He, A. Noble and V. K. Aggarwal, *J. Am. Chem. Soc.*, 2018, **140**, 10700–10704; (*f*) F. Sandfort, F. Strieth-Kalthoff, F. J. R. Klauck, M. J. James and F. Glorius, *Chem.–Eur. J.*, 2018, **24**, 17210–17214; (*g*) Y. Cheng, C. Mück-Lichtenfeld and A. Studer, *Angew. Chem., Int. Ed.*, 2018, **57**, 16832–16836; (*h*) J.-J. Zhang, X.-H. Duan, Y. Wu, J.-C. Yang and L.-N. Guo, *Chem. Sci.*, 2019, **10**, 161–166; (*i*) G. Yan, D. Huang and X. Wu, *Adv. Synth. Catal.*, 2018, **360**, 1040–1053.

26 *Lange's Handbook of Chemistry*, ed. J. A. Dean, McGraw-Hill, NewYork, NY, 15th edn, 1998.

27 L. Wang, T. Zhang, W. Sun, Z. He, C. Xia, Y. Lan and C. Liu, *J. Am. Chem. Soc.*, 2017, **139**, 5257.

28 A. Pelter, D. Buss, E. Colclough and B. Singaram, *Tetrahedron*, 1993, **49**, 7077–7103.

29 J. Metternich and R. Gilmour, *Synlett*, 2016, **27**, 2541–2552.

30 J.-J. Zhong, Q. Liu, C.-J. Wu, Q.-Y. Meng, X.-W. Gao, Z.-J. Li, B. Chen, C.-H. Tung and L.-Z. Wu, *Chem. Commun.*, 2016, **52**, 1800–1803.

31 (*a*) A. Fawcett, J. Pradeilles, Y. Wang, T. Mutsuga, E. L. Myers and V. K. Aggarwal, *Science*, 2017, **357**, 283–286; (*b*) D. Hu, L. Wang and P. Li, *Org. Lett.*, 2017, **19**, 2770–2773; (*c*) L. Candish, M. Teders and F. Glorius, *J. Am. Chem. Soc.*, 2017, **139**, 7440–7443; (*d*) Y. Cheng, C. Mück-Lichtenfeld and A. Studer, *J. Am. Chem. Soc.*, 2018, **140**, 6221–6225; (*e*) J. Wu, L. He, A. Noble and V. K. Aggarwal, *J. Am. Chem. Soc.*, 2018, **140**, 10700–10704; (*f*) Y. Cheng, C. Mück-Lichtenfeld and A. Studer, *Angew. Chem., Int. Ed.*, 2018, **57**, 16832–16836; (*g*) J.-J. Zhang, X.-H. Duan, Y. Wu, J.-C. Yang and L.-N. Guo, *Chem. Sci.*, 2019, **10**, 161–166; (*h*) G. Yan, D. Huang and X. Wu, *Adv. Synth. Catal.*, 2018, **360**, 1040–1053.